Biochemical Engineering Journal 117 (2017) 7–14

Contents lists available at ScienceDirect

Biochemical Engineering Journal

journal homepage: www.elsevier.com/locate/bej

Regular article

A reusable electrochemical biosensor for highly sensitive detection of mercury ions with an anionic intercalator supported on ordered mesoporous carbon/self-doped polyaniline nanofibers platform

Lin Tang[a,b,*], Xia Xie[a,b], Yaoyu Zhou[a,b,c], Guangming Zeng[a,b,*], Jing Tang[a,b], Yanan Wu[a,b], Beiqing Long[a,b], Bo Peng[a,b], Jingjing Zhu[a,b]

[a] College of Environmental Science and Engineering, Hunan University, Changsha, 410082, China
[b] Key Laboratory of Environmental Biology and Pollution Control (Hunan University), Ministry of Education, Changsha 410082, Hunan, China
[c] College of Resources and Environment, Hunan Agricultural University, Changsha, 410128, China

ARTICLE INFO

Article history:
Received 12 May 2016
Received in revised form
17 September 2016
Accepted 21 September 2016
Available online 23 September 2016

Keywords:
Reusable electrochemical biosensor
Mercury ions
Ordered mesoporous carbon
Self-doped polyaniline nanofibers
Anionic intercalator
Cysteine

ABSTRACT

In this paper, a reusable electrochemical biosensor was developed for highly sensitive detection of mercury ions (Hg^{2+}) using an anionic intercalator, which was based on Hg^{2+}-induced conformational change of a thymine-rich, single-stranded DNA (ssDNA) supported on the platform of ordered mesoporous carbon (OMC) and self-doped polyaniline (SPAN) nanofibers. In the presence of Hg^{2+}, the mercury-specific oligonucleotides were induced and folded into hairpin structure through mismatched thymine-Hg^{2+}-thymine (T-Hg^{2+}-T) base pairs from random coils. Then, the indicators intercalated into the hairpin structure and increased electric signal. OMC and SPAN nanofibers possessed excellent electrical conductivity which synergistically accelerated electron transfer and greatly improved the efficiency of electrochemical reaction at the electrode interface. Meanwhile, SPAN nanofibers strongly adhered to the electrode surface and attached rod-like OMC homogeneously and firmly, which provided a stable platform for DNA immobilization. Under the optimal conditions, the detection limit (LOD) for Hg^{2+} was 0.6 fM (S/N = 3). Furthermore, the biosensor could be easily regenerated by cysteine for cyclic utilization. Some environmental samples including lake sediment pore water and tap water were analyzed by the developed biosensor, the relatively satisfactory results indicated that it provided a green and promising strategy for detection of trace Hg^{2+} in the practical application.

1. Introduction

In recent decades, heavy metal pollution has been one of the most serious concerns because of their bioaccumulation and biotoxicity to human health and the ecological system. Particularly mercury, one of the most dangerous and highly toxic heavy metal pollutants, is widely distributed in the environment [1]. Mercury exists in various forms, such as divalent mercuric ion (Hg^{2+}), mercury sulfide (HgS), methylmercury (CH_3Hg^+) [2], of which the water-soluble mercuric ion is one of the most common and stable forms [3]. Long-term exposure to mercury in the environment and mercury accumulation in living organisms would cause a series of serious health problems such as kidney and liver damage, central nervous system defects, cardiomyopathy and arrhythmia, respiratory failure, endocrine disorders [4]. The world health organization (WHO) regulated that the total Hg^{2+} concentration in drinking water should be less than 0.001 mg/L [5]. Besides, pore water analyses could be used for toxicity identification and sediment quality assessment [6]. As a consequence, it is very important and significant to develop a simple, green, sensitive and low-cost sensor for quantitative determination of Hg^{2+} in the environment, especially in the aqueous media.

Many efforts were paid to develop various analytical methods for detection of Hg^{2+}. Traditional detection techniques include atomic absorption-emission spectroscopy [7], inductively coupled plasma mass spectrometry (ICP-MS) [8], cold vapor atomic fluorescence spectroscopy (CVAFS) [9], etc. While these methods have high sensitivity and accuracy, they generally require complicated and time-consuming sample preparation processes, professional operators, expensive and cumbersome machines and a large number of samples, which make them unsuitable for real-time detection to

* Corresponding authors at: College of Environmental Science and Engineering, Hunan University, Changsha, 410082, China.
E-mail addresses: tanglin@hnu.edu.cn (L. Tang), zgming@hnu.edu.cn (G. Zeng).

http://dx.doi.org/10.1016/j.bej.2016.09.011
1369-703X/

a large extent. In recent years, electrochemical sensors have been widely applied for detection of heavy metal ions, organic pollutants and biomolecules due to many advantages such as simplicity, portability, low cost and high sensitivity [10–13].

Since A. Ono and co-workers found that some base pairs could specifically bind to metal ions and form stable metal-mediated DNA duplexes, many sensors based on the metal-mediated base pairs were developed to detect metal ions [14,15]. It has been proved that Hg^{2+} can selectively coordinate with thymine (T) bases to form mismatched thymine-Hg^{2+}-thymine (T-Hg^{2+}-T) base pairs which are more stable than Watson-Crick A (adenine)-T pairs due to that the melting temperature (T_m) of the DNA duplexes containing T-T mispair in the presence of Hg^{2+} is higher than that of natural pair [16]. Recently, various approaches based on these unique properties have been developed to construct sensor platforms for targets detection by using advanced materials, such as quantum dots [17], metal nanoparticles [18], graphene [19], and carbon nanotubes [20]. Ordered mesoporous carbon (OMC) has attracted much attention since the first synthesis in 1999 [21]. Due to its well-ordered pore structure, high specific surface area, tunable pore diameters in the mesopore range as well as high thermal stability, flexible framework composition, electron transfer resistance and chemical inertness, OMC has been applied in catalysis [22], sensing [23,24], bioreactor construction [25], energy storage [26], etc. As one of the most promising conducting polymers, polyanilines (PAN) are also extensively applied in electrochemical sensors due to its specific properties, such as high electrical conductivity, good environmental stability and biocompatibility, facile synthesis, lower cost, homogeneity, special redox properties, and strong adherence to the electrode surface [27–30]. However, the conductivity of PAN will be significantly reduced when the pH of the solution is higher than 4 [31], which largely limits its application in biosensors. In order to overcome this drawback, self-doped polyanilines (SPAN), a type of polyaniline derivatives, have been widely prepared by chemical modification of polyanilines itself or chemical polymerization of appropriate monomers or electrochemical synthesis [32]. Compared with the parent PAN, SPAN with functional groups such as sulfonic and carboxylic acids, have their own unique properties. Especially, they can show good electric conductivity and electrochemical activity in an extended pH range. Therefore, SPAN can be widely applied to construct some biosensors that usually require neutral, slightly acidic or alkaline solutions due to the specificity of biomolecules such as DNA, RNA, enzyme, protein.

On the other hand, it is very important to choose a suitable signal indicator for improving the detection performance of electrochemical sensors. Of which, the label-free signal indicators have been widely applied in various sensors, especially DNA sensors, due to their good electrochemical performance and flexible, simple and stable features. In addition, cationic indicators such as methylene blue (MB) have a clear advantage with regards to intercalation rate, but would lead to a high background signal because of nonspecific adsorption in contrast with anionic indicators [33,34]. Therefore, the biosensors using anionic indicators could obtain better detection effects and lower detection limit due to the obviation of nonspecific adsorption. Disodium-anthraquinone-2, 6-disulfonate (AQDS), a kind of typical anionic indicators, was used for the proposed electrochemical biosensor.

In this paper, a kind of SPAN nanofibers was synthesized and applied to construct a reusable and sensitive electrochemical biosensor combining with OMC and using AQDS as the electric signal indicator for highly sensitive detection of Hg^{2+} based on the Hg^{2+}-induced conformational change of a thymine-rich, single-stranded DNA (ssDNA). SPAN nanofibers and OMC modified glassy carbon electrode (GCE) showed a remarkable capability of faster electron transfer and excellent stability. AQDS was selected as the electroactive signal indicator owing to its unique properties and good electrochemical performance. Gold nanoparticles (AuNPs) were electrodeposited on the SPAN/OMC modified electrode surface to immobilize mercury-specific oligonucleotides. Meanwhile, cysteine was used as a regenerant of the biosensor for cyclic utilization. Furthermore, in order to investigate the practical application ability, the constructed sensor was applied for detection of Hg^{2+} in lake sediment pore water and tap water.

2. Materials and methods

2.1. Chemicals and apparatus

OMC was synthesized as described previously in our laboratory [35–37]. Disodium-anthraquinone-2,6-disulfonate (AQDS) was purchased from Tokyo Chemical Industry Co., Ltd. (Tokyo, Japan). Hydrochloroauric acid ($HAuCl_4{\cdot}4H_20$) and aniline (AN) were purchased from Sinopharm Chemical Reagent Co., Ltd. (Shanghai, China). Tris(2-carboxyethyl)phosphine (TCEP), 6-Mercaptohexanol (MCH), tris(hydroxymethyl) aminomethane (Tris) and *N,N*-dimethylformamide (DMF) were purchased from Sigma-Aldrich (St. Louis, MO, USA). L-cysteine and all the other chemicals were of analytical grade and used as received. The preparation process of SPAN nanofibers was described in Section 1 of the Supplementary information (SI). The following buffer solutions were used in this study: DNA stock solution: 1 × TE buffer solution (pH 8.0); hybridization buffer solution: 10 mM Tris-HCl buffer solution (pH 7.0) containing 0.2 M NaCl; detection buffer solution: 50 mM phosphate buffer solutions (pH 7.0) containing 0.3 M NaCl (PBS); washing buffer solution: 10 mM Tris-HCl buffer solution (pH 7.0) containing 0.2 M NaCl (TBS). All solutions were prepared with ultrapure water (18 MΩ cm, Milli–Q, Millipore). The oligonucleotides were synthesized by Sangon (Shanghai, China) and purified by high-performance liquid chromatography, and the sequence of capture DNA probe was as follows: 5'-SH-$(CH_2)_6$-TTC TTT CTT CCCC TTG TTT GTT-3'.

Cyclic voltammetry (CV) measurements, differential pulse voltammetry (DPV) measurements and electrochemical impedance spectroscopy (EIS) measurements were carried on CHI760D electrochemical workstation (Chenhua Instrument, Shanghai, China). The conventional three-electrode system used in this work was made up of a modified glassy carbon electrode (GCE, 3 mm diameter) as the working electrode, a saturated calomel electrode (SCE) as the reference electrode and a Pt foil auxiliary electrode. Scanning electron microscopy (SEM) images of the materials were obtained by an S-4800 scanning electron microscope (Hitachi Ltd, Japan). High resolution transmission electron microscopy (HRTEM) images were obtained by a Tecnai G2 F20 S-TWIX electron microscope (FEI, Holland). An AFS-9700 atomic fluorescence spectrophotometer (Kechuang Haiguang Instrument, Beijing, China) was used to analyze environment samples for comparison with the proposed biosensor. A model PHSJ-3F laboratory pH meter (Leici Instrument, Shanghai, China) was employed for pH measurements of buffer solutions.

2.2. Preparation of the electrochemical Hg^{2+} biosensor

To construct the electrochemical Hg^{2+} biosensor, the bare GCE was carefully polished in alumina slurry at first. After rinsing with ultrapure water, the electrode was sonicated in acetone, ethanol and water successively. Then, the electrode was electrochemically treated in 0.5 M H_2SO_4 by cyclic voltammetry between −0.5 V and 1.5 V at 50 mV/s until a steady state redox curve was observed.

The self-assembled film was attached onto the GCE surface by layer-by-layer means. First, 5 μL SPAN nanofibers suspension (dispersed in DMF and ultrasonic processing before each use for

ensuring uniform distribution) was dropped onto the clean electrode surface, marked as the SPAN/GCE. After the electrode drying, 5 μL OMC suspension (dispersed in DMF) was dipcoated on the SPAN/GCE, and dried in the air to obtain the OMC/SPAN/GCE. Subsequently, to assemble capture DNA probes on the modified electrode, Au NPs were electrodeposited onto the OMC/SPAN/GEC surface by treating the modified electrode in 5 mL $HAuCl_4$ solution (1% wt) and 200 μL perchloric acid ($HClO_4$) at 0.2 V for 60 s, marked as the AuNPs/OMC/SPAN/GCE. Finally, 20 μL of 2 μM capture DNA probes (dissolved in TE buffer solution containing 0.1 mM TCEP and 1 M NaCl) were pipetted onto the AuNPs/OMC/SPAN/GCE surface and maintained at 4 °C for self-assembly through thiol–gold bonding (Au-S) for 12 h, marked as the DNA/AuNPs/OMC/SPAN/GCE. Rinsed with TBS buffer solution to remove non-specific adsorbed oligonucleotides, the modified electrode was immersed in 1 mM MCH ethanol solution for 30 min to form a MCH film to obtain a well-aligned DNA monolayer. Then, the prepared electrode was copiously rinsed with TBS buffer solution. When not in use, the biosensor obtained was stored in a moist state at 4 °C.

2.3. Electrochemical measurements

To detect Hg^{2+}, the biosensor was immersed into a series of different concentration of Hg^{2+} in hybridization buffer solution for 1 h at 37 °C, and then rinsed with TBS buffer solution. Subsequently, the biosensor was placed in AQDS solution for 6 h and then immersed into TBS buffer solution for 30 min and washed. Finally, DPV was performed in detection buffer solution between −0.7 V and −0.2 V with pulse amplitude of 50 mV, pulse width of 0.2 s and pulse period of 0.5 s. After detection of Hg^{2+}, the biosensor was regenerated by immersing the electrode into 10 mM Tris-HCl buffer solution (pH 7.0) containing 1 mM cysteine and 0.5 M NaCl for 3 h. Then washed with TBS buffer solution, the regenerated biosensor could be reused for another assay. All the measurements were performed at room temperature.

2.4. Environmental samples analysis

Two kinds of environmental samples, sediment pore water and tap water, were used for investigating the practical application ability of the proposed biosensor. The bottom sediment was obtained from Taozi Lake in Changsha, China and the sediment pore water was collected by suction filtration method. Then, the water samples were further filtered with 0.2 μm membrane to remove suspended substances and other organic impurities. The tap water samples were collected after being discharged about 30 min, and then boiled for 10 min to remove chlorine. Besides, the pH of all water samples was adjusted to 7.0 with Tris-HCl buffer solution before test with the biosensor. Finally, a series of samples with known different concentrations of Hg^{2+} were prepared by spiking. Meanwhile, the same water samples were analyzed by atomic fluorescence spectrometry (AFS) for comparison.

3. Results and discussion

3.1. Detection mechanism of the biosensor

The assemble process and detection strategy of the biosensor were shown in Scheme 1. In brief, SPAN nanofibers and OMC were dropped onto the clean GCE surface by layer-by-layer self-assembly. Au NPs were electrodeposited on the modified electrode surface mainly to immobilize capture DNA probes due to the formation of the stable Au-S, which also contributed to accelerating electron transfer. After treatment with MCH to remove nonspecific adsorption of DNA on the electrode surface and to make the DNA monolayers well aligned [38], the mercury-specific oligonucleotides were immobilized onto the electrode surface via self-assembly through thiol anchor to obtain the electrochemical Hg^{2+} biosensor. In the presence of Hg^{2+}, the ssDNA probes were induced and folded into hairpin structure by T-T mismatch with Hg^{2+}. Then, AQDS intercalated into the hairpin structure and clearly increased the electric signal. Here, AQDS was used as the electric signal indicator because it has a unique anthracene ring structure which could be selectively embedded in the duplex structure of double-stranded DNA (dsDNA) and show a good electrochemical activity due to a reversible 2-electron transfer process for its quinone/hydroquinone redox couple in electrochemistry (Fig. S1, SI) [39]. The electrical signal will change with the change of DNA conformation. In addition, AQDS is a kind of anionic indicator which contributes to decreasing electrostatic attraction between DNA and indicator, thereby reducing background signal [40]. However, Hg^{2+} was easily separated from the T-Hg^{2+} –T complexes after immersing the biosensor into cysteine solution due to the formation of Hg-SR bond between Hg^{2+} and cysteine that is more

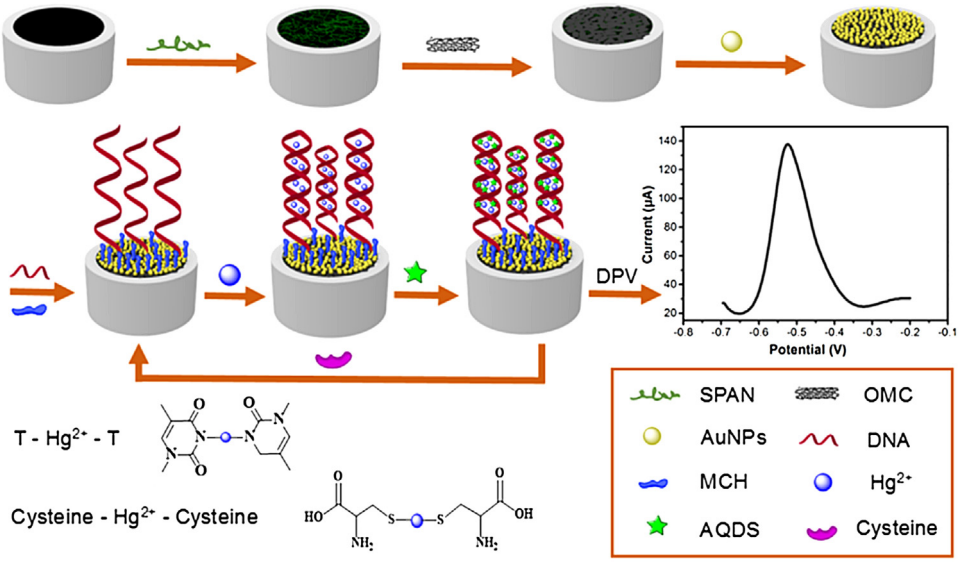

Scheme 1. Assemble process and schematic diagram of the biosensor for detection of Hg^{2+}.

stable than T-Hg^{2+}-T structure, which led to recovery of free-state single-stranded oligonucleotides from hairpin structure [41–43]. Therefore, the biosensor could be easily regenerated by immersing it in the cysteine solution.

3.2. Morphology characterization of SPAN nanofibers and OMC

The morphology characterization of SPAN nanofibers and OMC was investigated by scanning electron microscopy (SEM) and high resolution transmission electron microscopy (HRTEM). Fig. 1a showed that SPAN nanofibers were interconnected through many nods to form a net-like or ring-like structure with a uniform diameter between 50 nm and 60 nm, which can attach rod-like OMC on the electrode surface uniformly and firmly. In addition, the Fourier transform infrared (FT-IR) spectrum of SPAN nanofibers was shown in Fig. S2 of the Supplementary information, which indicated that SPAN nanofibers contained abundant functional groups and contributed to SPAN nanofibers strongly adhering to the GCE surface and providing sufficient binding sites for adhesion of OMC. Fig. 1b showed that OMC was in the form of rod-like morphology, and the average length was about 500 nm to 1 μm. Besides, from the HRTEM image of Fig. 1c, a highly ordered stripe-like structure can be observed clearly. In order to further investigate the morphologies of the bare GCE and the different modified electrodes, the SEM images were shown in Fig. S3 of the Supplementary information.

3.3. Electrochemical behavior of the modified electrodes

Electrochemical impedance spectroscopy (EIS) was employed to investigate the impedance change of the electrode surface in the process of modification and provide more information about interface assembly. The measured impedance data can be fitted with an assumed equivalent circuit model, thereby extracting equivalent values of resistances and capacitances [44]. As the inset shown in Fig. 2a, one of common equivalent circuit models is composed of four equivalent circuit elements including solution resistance (R_s), interfacial capacitance (C_{dl}), charge transfer resistance (R_{ct}) and warburg impedance (Z_w) [45,46]. The nyquist plot of EIS contains a semicircle part at higher frequencies representing for charge transfer resistance which dominates the electron transfer kinetics of redox probe at the electrode interface, and a linear part at lower frequencies representing for diffusion process [47]. Here, this model was applied to fit the measured impedance data of the different modified electrodes. From Fig. S4, Fig. S5 and Fig. S6 of the Supplementary information, the good fitting results (the fitting errors for each equivalent circuit elements were less than 5%) between the measured data and the fitting curves indicated that this equivalent circuit model was appropriate for this electrochemical system. Of which, the equivalent circuit element values of the different modified were shown in Table S1 (SI). Fig. 2a exhibited the nyquist plots of the different modified electrodes in 5.0 mM $[Fe(CN)_6]^{3-/4-}$ (1:1) solution containing 0.1 M KCl at open circuit potential with frequency varied from 0.01 Hz to 10^5 Hz. As can be seen, the bare GCE had a maximum R_{ct} with 1110 Ω (curve a, Table S1, SI), and after self-assembly of SPAN nanofibers, the value of R_{ct} decreased to 424.6 Ω (curve b, Table S1, SI), which indicated that SPAN nanofibers could promote electron transfer at the electrode interface. However, compared with AuNPs/GCE with R_{ct} 258.4 Ω (curve c, Table S1, SI) and OMC/GCE with R_{ct} 93.26 Ω (curve d, Table S1, SI), the nyquist plots presented an almost straight line after the modification of OMC and AuNPs successively with the values of R_{ct} further decreasing to 16 Ω (curve e, Table S1, SI) and 5.108 Ω (curve f, Table S1, SI) respectively, which was attributed to the superior electrical conductivity of OMC and AuNPs as well as their synergistic effect in facilitating the electron transfer between $[Fe(CN)_6]^{3-/4-}$

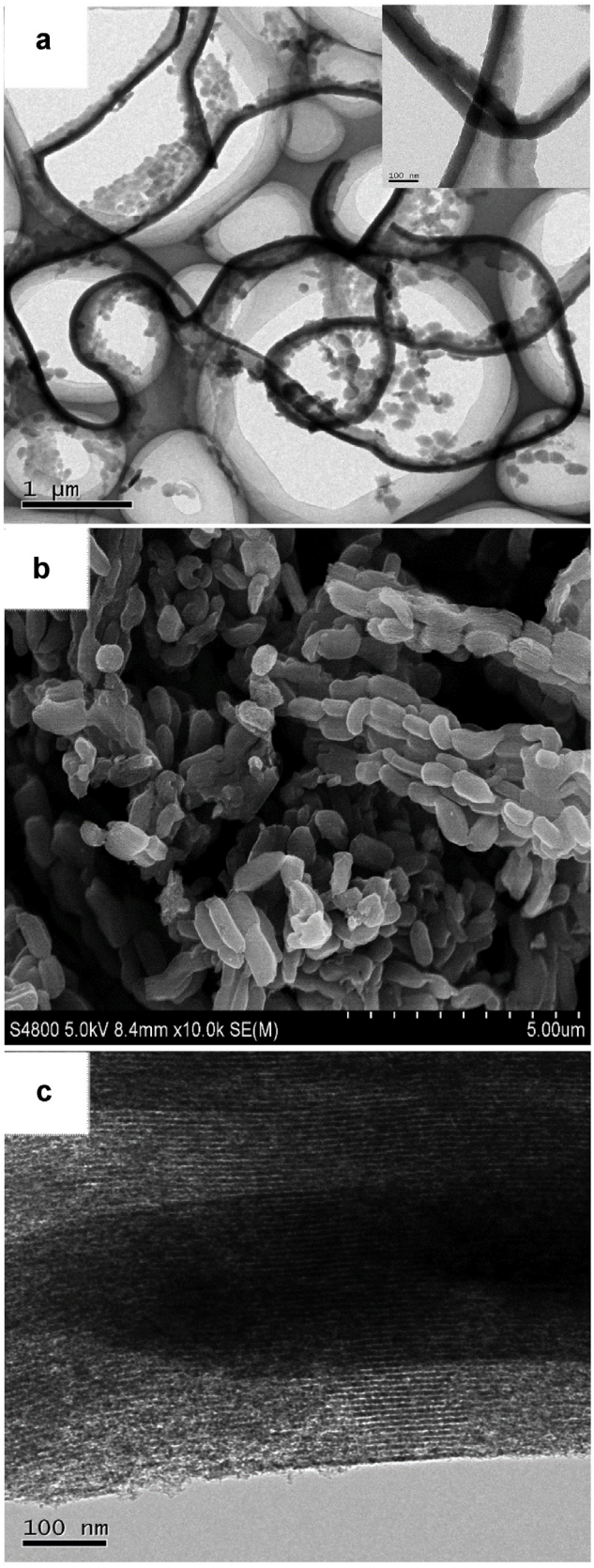

Fig. 1. **a** HRTEM image of SPAN nanofibers; **b** SEM image of OMC; **c** HRTEM image of OMC.

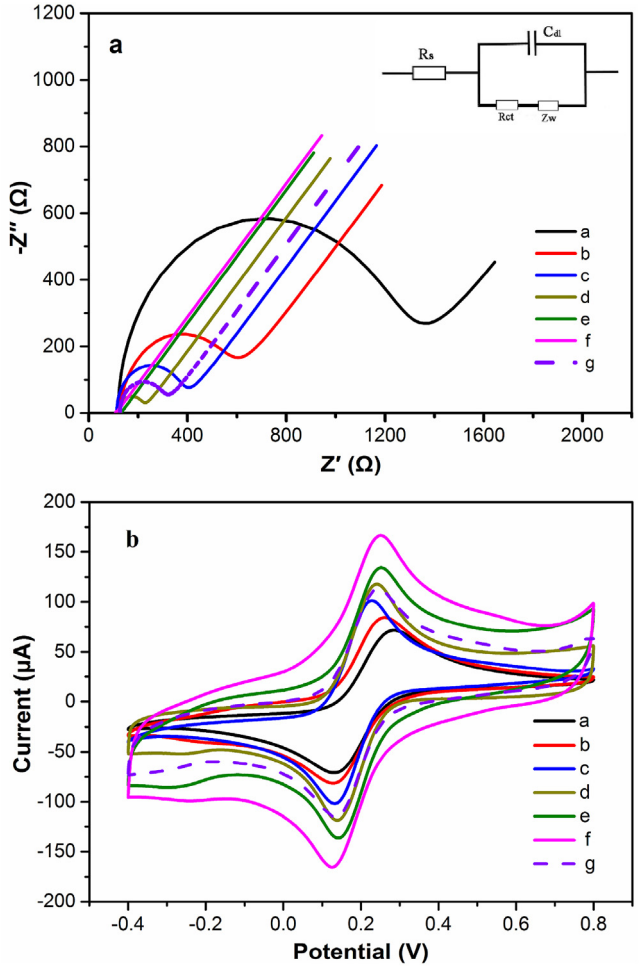

Fig. 2. a Electrochemical impedance spectra (Nyquist plots) of the bare GCE (a), SPAN/GCE (b), AuNPs/GCE (c), OMC/GCE (d), OMC/SPAN/GCE (e), AuNPs/OMC/SPAN/GCE (f) and DNA/AuNPs/OMC/SPAN/GCE (g) with frequency range from 0.01 Hz to 10^5 Hz; **b** cyclic voltammograms (CVs) of the bare GCE (a), SPAN/GCE (b), AuNPs/GCE (c), OMC/GCE (d), OMC/SPAN/GCE (e), AuNPs/OMC/SPAN/GCE (f) and DNA/AuNPs/OMC/SPAN/GCE (g) in 5.0 mM $[Fe(CN)_6]^{3-/4-}$ (1:1) solution containing 0.1 M KCl at the scan rate of 50 mV/s.

and the modified electrodes surface. However, the value of R_{ct} significantly increased to 172.1 Ω (curve g, Table S1, SI) after being self-assembled with DNA probes. The reason for that might be the repellence of redox probe from approaching electrode surface by negative charged phosphate skeletons of DNA. At the same time, it could be concluded that DNA probes were successfully immobilized on the modified electrode surface.

To further monitor the modification process of the electrode, cyclic voltammetry (CV) was carried out in 5.0 mM $[Fe(CN)_6]^{3-/4-}$ (1:1) solution containing 0.1 M KCl at the scan rate of 50 mV/s to test the electrochemical properties of the different modified electrodes. Cyclic voltammograms were shown in Fig. 2b, and as can be seen, well defined redox peaks were obtained. Besides, obviously, the current signals of SPAN/GCE (curve b), AuNPs/GCE (curve c) and OMC/GCE (curve d) were enhanced compared with the bare GCE (curve a), which were attributed to the larger electroactive surface areas and better electron transfer ability of these materials. However, after OMC being attached on the SPAN/GCE, the redox peak currents (curve e) increased compared with the above. Furthermore, after AuNPs being electrodeposited on the OMC/SPAN/GCE, the redox peak currents (curve f) were obviously higher than the OMC/SPAN/GCE. The reason for that might be owing to the better electron transfer ability of these materials and

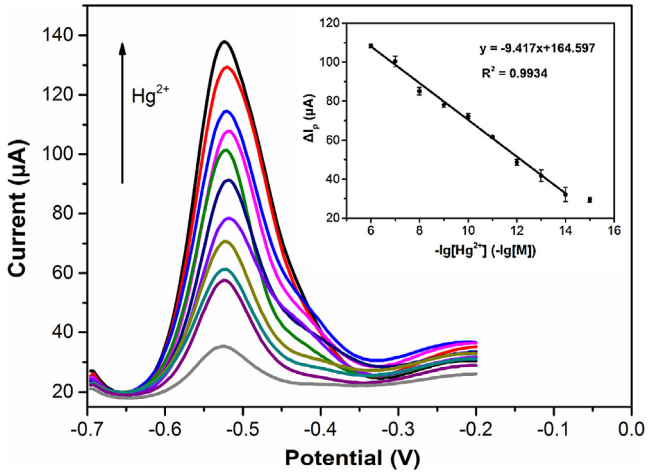

Fig. 3. DPV responses of the biosensor at different concentrations of Hg^{2+} solution (from top to bottom: 1 μM, 100 nM, 10 nM, 1 nM, 100 pM, 10 pM, 1 pM, 100 fM, 10 fM, 1 fM and 0 M); Inset: the linear relationship between the peak current change and the negative logarithm of Hg^{2+} concentration. The error bars indicated standard deviations from three replicative tests.

the synergistic amplification effect between them, thereby accelerating the electron transfer of $[Fe(CN)_6]^{3-/4-}$ on the electrode surface. On the other hand, the composite membrane comprising of SPAN nanofibers, OMC and AuNPs modified on the electrode surface enlarged the microscopic electroactive area and improved the charge transport efficiency of $[Fe(CN)_6]^{3-/4-}$. Meanwhile, the AuNPs/OMC/SPAN/GCE also exhibited excellent stability (Fig. S7, SI) and repeatability (Fig. S8, SI) for electrochemical performance, which provided a good platform for immobilization of DNA to construct a biosensor. After DNA probes being self-assembled on the AuNPs/OMC/SPAN/GCE, the redox peak currents decreased obviously (curve g). The cyclic voltammograms indicated that the modified electrode had a good current response performance.

3.4. Response of the biosensor to Hg^{2+}

The sensitivity of the biosensor was investigated by differential pulse voltammetry (DPV) with the use of AQDS as the electric signal indicator in case of varying Hg^{2+} concentration. Fig. 3 showed the DPV responses of the biosensor to Hg^{2+} at different concentrations under optimal experimental conditions (Fig. S9, SI). Obviously, the peak current increased with the increase of Hg^{2+} concentrations, which was attributed to the increase of the T-Hg^{2+}-T complexes and more AQDS molecules intercalating into the duplex structure of dsDNA and resulting in electric signal enhancement. As shown in the inset of Fig. 3, a linear relationship between the peak current difference values and the negative logarithm value of Hg^{2+} concentration was obtained as follows.

$$Y = -9.417X + 164.597$$

in which, Y represented the difference value of the peak current value and the blank value, X represented the negative logarithm value of Hg^{2+} concentration. The correlation coefficient of the linear regression equation is 0.9934. The biosensor exhibited a relatively wide detection linear range from 10 fM to 1 μM with a low detection limit (LOD) of 0.6 fM (S/N = 3). Compared with some of the other analytical methods, the proposed biosensor exhibited significantly improved analytical performances in terms of linear detection range and detection limit. Table 1 listed the performances of some biosensors reported for detection of Hg^{2+}.

Table 1
Comparison of some biosensors reported for detection of Hg^{2+}.

Detection methods	Materials	Linear ranges	Detection limits	References
Fluorescence detection	CdS/ZnS Quantum Dots (CdS/ZnS QDs), AuNPs	1.0–10 nM	0.18 nM	[16]
Electrochemical detection	AuNPs	1–100 nM	0.5 nM	[17]
Electrochemical detection	Single Walled Carbon Nanotubes (SWCNTs)	0.1–1.0 pM	16.3 fM	[19]
Colorimetric detection	Cationic polymer	0.25–500 nM	0.15 nM	[48]
Fluorescence detection	Au nanoclusters (Au NCs)	1–20 nM	0.5 nM	[49]
Surface-enhanced Raman scattering (SERS) detection	AuNPs, reduced graphene oxide (rGO)	Not reported	0.1 nM	[50]
Fluorescence detection	Silver nanoclusters (Ag NCs)	10–300 nM	10 nM	[51]
Electrochemical detection	Auelectrode	0.1–100 nM	0.03 nM	[52]
Electrochemical detection	Au electrode	0.1 nM–5 μM	0.06 nM	[53]
Electrochemical detection	SPAN nanofibers, OMC, AuNPs	10 fM–1 μM	0.6 fM	This work

3.5. Selectivity, regeneration, reproducibility, repeatability and stability of the biosensor

For investigating the anti-jamming capability of the developed Hg^{2+} biosensor, some potential interfering ions which may exist in environmental samples, such as K^+, Pb^{2+}, Cd^{2+}, Cu^{2+}, Zn^{2+}, Ca^{2+}, Mg^{2+}, Co^{2+}, Cr^{3+}, Al^{3+}, were tested at the concentrations of 1 μM. The results were described in Fig. 4. As can be seen, except for Hg^{2+} and mixed solution containing Hg^{2+}, the biosensor exhibited poor current responses to the other metal ions, and it was obvious that the largest current change was induced by Hg^{2+}, which was consistent with the specific T-Hg^{2+}-T coordination chemistry. The test results indicated that the proposed biosensor possessed a promising and relatively satisfactory capacity of resisting disturbance toward Hg^{2+}.

It is very important for the regeneration of aptamer-based sensors in their practical application. In this work, taking full advantage of cysteine that could disrupt the formative hairpin structure through T-T mismatch with Hg^{2+}, the biosensor was regenerated by treating with solution containing cysteine. As shown in Fig. 5, after 10 cycle tests, the blank signal of the biosensor almost remained unchanged and the response signal to the same concentration Hg^{2+} only slightly decreased. It indicated that the biosensor can be readily regenerated by immersing the electrode into the solution containing cysteine under appropriate conditions.

The reproducibility of the biosensor was performed by repetitive measurements (n = 5) using five independently modified electrodes for detection of 1 μM and 10 pM of Hg^{2+} respectively through above mentioned procedures and conditions. As shown in Fig. S10 (SI), the DPV response curves exhibited satisfactory reproducibility with the relative standard deviations (RSDs) of 1.91% for 1 μM of Hg^{2+} and 2.49% for 10 pM of Hg^{2+}.

The repeatability of the biosensor was investigated by successive detection of 1 μM and 10 pM of Hg^{2+} respectively using the same modified electrode under the above mentioned conditions. As shown in Fig. S11 (SI), the DPV response curves exhibited good coincidence with the RSDs of 2.07% for 1 μM of Hg^{2+} 1.99% for 10 pM of Hg^{2+}, indicating good repeatability.

The storage stability of the biosensor was investigated by measuring DPV responses to 1 μM and 10 pM of Hg^{2+} after being kept in a moist state at 4 °C for a certain time. As shown in Fig. S12 (SI), it turned out that 82.34% for 1 μM of Hg^{2+} and 85.19% for 10 pM of Hg^{2+} of the original peak currents were remained after one month, which indicated that the proposed biosensor has relatively good stability.

3.6. Analysis of Hg^{2+} in environmental samples

To test the practicality of the proposed biosensor, a series of experiments were carried out to detect Hg^{2+} in environmental samples including sediment pore water samples and tap water samples. After pretreatment, all the water samples with different known concentrations of Hg^{2+} were analyzed by the proposed biosensor and atomic fluorescence spectrometry (AFS). The detection results were shown in Table 2. Obviously, the detection results of the biosensor and AFS were basically consistent. Furthermore, compared with the AFS, the biosensor overcame some drawbacks such as complex sample pretreatment process, expensive instruments

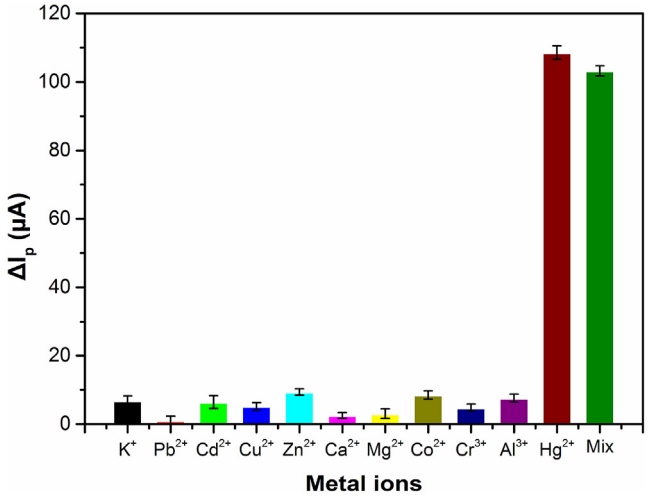

Fig. 4. Selectivity of the Hg^{2+} biosensor: 1 μM of Hg^{2+}, 1 μM of K^+, Pb^{2+}, Cd^{2+}, Cu^{2+}, Zn^{2+}, Ca^{2+}, Mg^{2+}, Co^{2+}, Cr^{3+}, Al^{3+} and their mixture containing 1 μM of Hg^{2+} were respectively tested under the optimal experimental conditions. The error bars indicated standard deviations from three replicative tests.

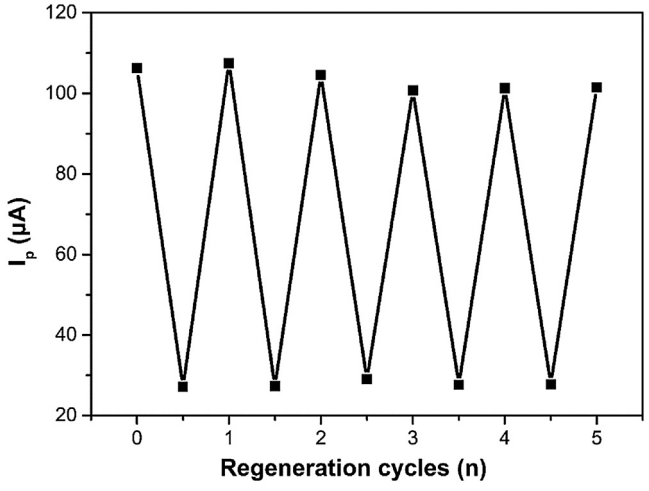

Fig. 5. Regeneration of the biosensor with the stepwise interaction with Hg^{2+} (1 nM) and cysteine.

Table 2
Detection of Hg^{2+} in environmental samples by the biosensor and AFS.

Samples	Original concentration[a] (nM)	Concentration added (nM)	Measured concentration[b] (nM)		Relative deviation (%)
			The biosensor	AFS	
Sediment pore water	0.2 ± 0.1	5	5.1 ± 0.5	5.0 ± 0.4	2.0
		10	10.4 ± 0.2	10.0 ± 0.4	4.0
		20	20.4 ± 0.3	20.8 ± 0.6	1.9
Tap water	Not found	5	4.6 ± 0.8	4.8 ± 0.7	4.2
		10	10.1 ± 0.8	10.3 ± 0.3	1.9
		20	20.0 ± 0.6	20.6 ± 0.3	2.9

[a,b]An average of three replicate measurements. The original concentration was measured by AFS.

and great consumption of reagents. From the above, the proposed biosensor has good application potential in the real environmental samples.

4. Conclusions

An ultrasensitive and reusable electrochemical DNA biosensor has been constructed for highly sensitive detection of Hg^{2+} using DNA anionic intercalator as signal indicator based on ordered mesoporous carbon/self-doped polyaniline nanofibers composites modified glassy carbon electrode. The proposed biosensor exhibited an excellent linear range and low detection limit. Furthermore, the proposed biosensor showed lots of superior performances such as good stability, repeatability and reproducibility. Those good properties of the biosensor mainly count on the following respects: (1) the synergistic amplification effect of SPAN nanofibers, OMC and AuNPs significantly contributed to accelerating the electron transfer on the modified electrode surface, thereby enhancing the sensitivity of the biosensor; (2) the composite membrane comprising of SPAN nanofibers, OMC and AuNPs modified electrode provided a good and stable platform for the mercury-specific oligonucleotides immobilization, which was beneficial to increase stability of the biosensor; (3) AQDS, a kind of DNA anionic intercalator was used as the signal indicator and decreased electrostatic adsorption between DNA and indicators, thereby reducing background signal of the biosensor; (4) Unique T-Hg^{2+}-T coordination chemistry made sure the selectivity and high sensitivity of the biosensing system. In addition, the biosensor could be regenerated by treating with the solution containing cysteine. The relatively satisfactory experimental results indicated that the proposed biosensor had a potential application in real environmental samples monitoring, and the similar assembly method could also be extended to construct some new sensors based on hairpin-structured oligonucleotides and intercalators for detection of some other corresponding heavy metals ions.

Acknowledgments

The study was financially supported by the National Program for Support of Top–Notch Young Professionals of China (2012), Projects 51579096, 51222805, 51521006 and 51508175 supported by National Natural Science Foundation of China, the Program for New Century Excellent Talents in University from the Ministry of Education of China (NCET–11–0129), and the Hunan Province Innovation Foundation for Postgraduate (No. CX2015B095).

Appendix A. Supplementary data

Supplementary data associated with this article can be found, in the online version, at http://dx.doi.org/10.1016/j.bej.2016.09.011.

More information included the preparation of SPAN nanofibers, the cyclic voltammograms (CVs) of the biosensor with AQDS and without AQDS, the FT-IR spectrum of SPAN nanofibers, the morphology characterization of the bare GCE and the different modified electrodes, the electrochemical characterization of the modified electrode, the optimization of detection conditions, and the reproducibility, repeatability and stability of the biosensor.

References

[1] P.B. Tchounwou, W.K. Ayensu, N. Ninashvili, D. Sutton, Environmental exposure to mercury and its toxicopathologic implications for public health, Environ. Toxicol. 18 (2003) 149–175.
[2] F. Cai, Q. Zhu, K. Zhao, A. Deng, J. Li, Multiple signal amplified electrochemiluminescent immunoassay for Hg^{2+} using graphene-coupled quantum dots and gold nanoparticles-labeled horseradish peroxidase, Environ. Sci. Technol. 49 (2015) 5013–5020.
[3] L.D. Hylander, M.E. Goodsite, Environmental costs of mercury pollution, Sci. Total Environ. 368 (2006) 352–370.
[4] J.W. Sekowski, L.H. Malkas, Y. Wei, R.J. Hickey, Mercuric ion inhibits the activity and fidelity of the human cell DNA synthesome, Toxicol. Appl. Pharmacol. 145 (1997) 268–276.
[5] J. Duruibe, M. Ogwuegbu, J. Egwurugwu, Heavy metal pollution and human biotoxic effects, Int. J. Phys. Sci. 2 (2007) 112–118.
[6] S.E. Bufflap, H.E. Allen, Sediment pore water collection methods for trace metal analysis: a review, Water Res. 29 (1995) 165–177.
[7] N.H. Bings, A. Bogaerts, J.A.C. Broekaert, Atomic spectroscopy, Anal. Chem. 78 (2006) 3917–3946.
[8] S. Ashoka, B.M. Peake, G. Bremner, K.J. Hageman, M.R. Reid, Comparison of digestion methods for ICP-MS determination of trace elements in fish tissues, Anal. Chim. Acta 653 (2009) 191–199.
[9] A.W. Rea, G.J. Keeler, Microwave digestion and analysis of foliage for total mercury by cold vapor atomic fluorescence spectroscopy, Biogeochemistry 40 (1998) 115–123.
[10] C. Zhang, C. Lai, G. Zeng, D. Huang, L. Tang, C. Yang, Y. Zhou, L. Qin, M. Cheng, Nanoporous Au-based chronocoulometric aptasensor for amplified detection of Pb using DNAzyme modified with Au nanoparticles, Biosens. Bioelectron. 81 (2016) 61–67.
[11] L. Tang, G.-M. Zeng, G.-L. Shen, Y.-P. Li, Y. Zhang, D.-L. Huang, Rapid detection of picloram in agricultural field samples using a disposable immunomembrane-based electrochemical sensor, Environ. Sci. Technol. 42 (2008) 1207–1212.
[12] Y. Zhang, G.M. Zeng, L. Tang, D.L. Huang, X.Y. Jiang, Y.N. Chen, A hydroquinone biosensor using modified core-shell magnetic nanoparticles supported on carbon paste electrode, Biosens. Bioelectron. 22 (2007) 2121–2126.
[13] Z. Li, X. Miao, A. Zhu, L. Ling, Hybridization chain reaction and gold nanoparticles dual signal amplification for sensitive glucose detection, Biochem. Eng. J. 103 (2015) 205–210.
[14] A. Ono, S. Cao, H. Togashi, M. Tashiro, T. Fujimoto, T. Machinami, S. Oda, Y. Miyake, I. Okamoto, Y. Tanaka, Specific interactions between silver(I) ions and cytosine-cytosine pairs in DNA duplexes, Chem. Commun. (2008) 4825–4827.
[15] A. Ono, H. Togashi, Highly selective oligonucleotide-based sensor for mercury(II) in aqueous solutions, Angew. Chem. 43 (2004) 4300–4302.
[16] Y. Miyake, H. Togashi, M. Tashiro, H. Yamaguchi, S. Oda, M. Kudo, Y. Tanaka, Y. Kondo, R. Sawa, T. Fujimoto, Mercury(II)-mediated formation of thymine-Hg(II)-thymine base pairs in DNA duplexes, J. Am. Chem. Soc. 128 (2006) 2172–2173.
[17] D. Huang, C. Niu, X. Wang, X. Lv, G. Zeng, Turn-on fluorescent sensor for Hg^{2+} based on single-stranded DNA functionalized Mn:CdS/ZnS quantum dots and gold nanoparticles by time-gated mode, Anal. Chem. 85 (2013) 1164–1170.
[18] R.M. Kong, X.B. Zhang, L.L. Zhang, X.Y. Jin, S.Y. Huan, G.L. Shen, R.Q. Yu, An ultrasensitive electrochemical turn-on label-free biosensor for Hg^{2+} with AuNP-functionalized reporter DNA as a signal amplifier, Chem. Commun. (2009) 5633–5635.
[19] Y. Zhang, G.M. Zeng, L. Tang, J. Chen, Y. Zhu, X.X. He, Y. He, Electrochemical sensor based on electrodeposited graphene-Au modified electrode and NanoAu carrier amplified signal strategy for attomolar mercury detection, Anal. Chem. 87 (2015) 989–996.

[20] L. Guo, N. Yin, D. Nie, F. Fu, G. Chen, An ultrasensitive electrochemical sensor for the mercuric ion via controlled assembly of SWCNTs, Chem. Commun. 47 (2011) 10665–10667.
[21] R. Ryoo, S.H. Joo, S. Jun, Synthesis of highly ordered carbon molecular sieves via template-mediated structural transformation, J. Phys. Chem. B 103 (1999) 7743–7746.
[22] M. Zhou, J. Ding, L.-p. Guo, Q.-k. Shang, Electrochemical behavior of L-cysteine and its detection at ordered mesoporous carbon-modified glassy carbon electrode, Anal. Chem. 79 (2007) 5328–5335.
[23] L. Tang, J. Chen, G. Zeng, Y. Zhu, Y. Zhang, Y. Zhou, X. Xie, G. Yang, S. Zhang, Ordered mesoporous carbon and thiolated polyaniline modified electrode for simultaneous determination of Cadmium(II) and Lead(II) by anodic stripping voltammetry, Electroanalysis 26 (2014) 2283–2291.
[24] J. Dong, Y. Hu, S. Zhu, J. Xu, Y. Xu, A highly selective and sensitive dopamine and uric acid biosensor fabricated with functionalized ordered mesoporous carbon and hydrophobic ionic liquid, Anal. Bioanal. Chem. 396 (2010) 1755–1762.
[25] M. Hartmann, Ordered mesoporous materials for bioadsorption and biocatalysis, Chem. Mater. 17 (2005) 4577–4593.
[26] J. Lee, J. Kim, T. Hyeon, Recent progress in the synthesis of porous carbon materials, Adv. Mater. 18 (2006) 2073–2094.
[27] D. Zhai, B. Liu, Y. Shi, L. Pan, Y. Wang, W. Li, R. Zhang, G. Yu, Highly sensitive glucose sensor based on pt nanoparticle/polyaniline hydrogel heterostructures, ACS Nano 7 (2013) 3540–3546.
[28] W. Tang, M. Zhang, W. Li, X. Zeng, An electrochemical sensor based on polyaniline for monitoring hydroquinone and its damage on DNA, Talanta 127 (2014) 262–268.
[29] S. Chawla, R. Rawal, S. Sharma, C.S. Pundir, An amperometric biosensor based on laccase immobilized onto nickel nanoparticles/carboxylated multiwalled carbon nanotubes/polyaniline modified gold electrode for determination of phenolic content in fruit juices, Biochem. Eng. J. 68 (2012) 76–84.
[30] R. Devi, S. Yadav, C.S. Pundir, Electrochemical detection of xanthine in fish meat by xanthine oxidase immobilized on carboxylated multiwalled carbon nanotubes/polyaniline composite film, Biochem. Eng. J. 58-59 (2011) 148–153.
[31] C.M.A. Brett, C. Thiemann, Conducting polymers from aminobenzoic acids and aminobenzenesulphonic acids: influence of pH on electrochemical behaviour, J. Electroanal. Chem. 538 (2002) 215–222.
[32] A. Malinauskas, Self-doped polyanilines, J. Power Sources 126 (2004) 214–220.
[33] E.L.S. Wong, P. Erohkin, J.J. Gooding, A comparison of cationic and anionic intercalators for the electrochemical transduction of DNA hybridization via long range electron transfer, Electrochem. Commun. 6 (2004) 648–654.
[34] Y. Zhou, L. Tang, G. Zeng, C. Zhang, Y. Zhang, X. Xie, Current progress in biosensors for heavy metal ions based on DNAzymes/DNA molecules functionalized nanostructures: a review, Sens. Actuators B 223 (2016) 280–294.
[35] L. Tang, Y. Zhou, G. Zeng, Z. Li, Y. Liu, Y. Zhang, G. Chen, G. Yang, X. Lei, M. Wu, A tyrosinase biosensor based on ordered mesoporous carbon-Au/L-lysine/Au nanoparticles for simultaneous determination of hydroquinone and catechol, Analyst 138 (2013) 3552–3560.
[36] Y. Zhou, L. Tang, G. Zeng, J. Chen, Y. Cai, Y. Zhang, G. Yang, Y. Liu, C. Zhang, W. Tang, Mesoporous carbon nitride based biosensor for highly sensitive and selective analysis of phenol and catechol in compost bioremediation, Biosens. Bioelectron. 61 (2014) 519–525.
[37] Y. Zhou, L. Tang, G. Zeng, J. Chen, J. Wang, C. Fan, G. Yang, Y. Zhang, X. Xie, Amplified and selective detection of manganese peroxidase genes based on enzyme-scaffolded-gold nanoclusters and mesoporous carbon nitride, Biosens. Bioelectron. 65C (2014) 382–389.
[38] P. Miao, K. Han, B. Wang, G. Luo, P. Wang, M. Chen, Y. Tang, Electrochemical detection of aqueous Ag^{+} based on Ag^{+}-assisted ligation reaction, Sci. Rep 5 (2015) 9161.
[39] E.L. Wong, J.J. Gooding, Electronic detection of target nucleic acids by a 2, 6-disulfonic acid anthraquinone intercalator, Anal. Chem. 75 (2003) 3845–3852.
[40] Y. Zhou, L. Tang, G. Zeng, J. Zhu, H. Dong, Y. Zhang, X. Xie, J. Wang, Y. Deng, A novel biosensor for silver(I) ion detection based on nanoporous gold and duplex-like DNA scaffolds with anionic intercalator, RSC Adv. 5 (2015) 69738–69744.
[41] H. Xu, M. Hepel, Molecular beacon-based fluorescent assay for selective detection of glutathione and cysteine, Anal. Chem. 83 (2011) 813–819.
[42] S.M. Jia, X.F. Liu, P. Li, D.M. Kong, H.X. Shen, G-quadruplex DNAzyme-based Hg^{2+} and cysteine sensors utilizing Hg^{2+}-mediated oligonucleotide switching, Biosens. Bioelectron. 27 (2011) 148–152.
[43] J.S. Lee, P.A. Ulmann, M.S. Han, C.A. Mirkin, A DNA-gold nanoparticle-based colorimetric competition assay for the detection of cysteine, Nano Lett. 8 (2008) 529–533.
[44] J.S. Daniels, N. Pourmand, Label-Free impedance biosensors: opportunities and challenges, Electroanalysis 19 (2007) 1239–1257.
[45] Y. Zhou, L. Tang, X. Xie, G. Zeng, J. Wang, Y. Deng, G. Yang, C. Zhang, Y. Zhang, J. Chen, Sensitive impedimetric biosensor based on duplex-like DNA scaffolds and ordered mesoporous carbon nitride for silver(I) ion detection, Analyst 139 (2014) 6529–6535.
[46] A. Patolsky, Electronic transduction of DNA sensing processes on surfaces: amplification of DNA detection and analysis of single-aase mismatches by tagged liposomes, J. Am. Chem. Soc. 123 (2001) 5194–5205.
[47] P. Du, H. Li, Z. Mei, S. Liu, Electrochemical DNA biosensor for the detection of DNA hybridization with the amplification of Au nanoparticles and CdS nanoparticles, Bioelectrochemistry 75 (2009) 37–43.
[48] Y. Zhu, Y. Cai, Y. Zhu, L. Zheng, J. Ding, Y. Quan, L. Wang, B. Qi, Highly sensitive colorimetric sensor for Hg^{2+} detection based on cationic polymer/DNA interaction, Biosens. Bioelectron. 69 (2015) 174–178.
[49] J. Xie, Y. Zheng, J.Y. Ying, Highly selective and ultrasensitive detection of Hg^{2+} based on fluorescence quenching of Au nanoclusters by Hg^{2+}-Au^{+} interactions, Chem. Commun. 46 (2010) 961–963.
[50] X. Ding, L. Kong, J. Wang, F. Fang, D. Li, J. Liu, Highly sensitive SERS detection of Hg^{2+} ions in aqueous media using gold nanoparticles/graphene heterojunctions, ACS Appl. Mater. Interfaces 5 (2013) 7072–7078.
[51] L. Deng, Z. Zhou, J. Li, T. Li, S. Dong, Fluorescent silver nanoclusters in hybridized DNA duplexes for the turn-on detection of Hg^{2+} ions, Chem. Commun. 47 (2011) 11065–11067.
[52] L. Chen, Z.N. Chen, A multifunctional label-free electrochemical impedance biosensor for Hg^{2+}, adenosine triphosphate and thrombin, Talanta 132 (2015) 664–668.
[53] D. Wu, Q. Zhang, X. Chu, H. Wang, G. Shen, R. Yu, Ultrasensitive electrochemical sensor for mercury(II) based on target-induced structure-switching DNA, Biosens. Bioelectron. 25 (2010) 1025–1031.